

Determination by x-ray reflectivity and small angle x-ray scattering of the porous properties of mesoporous silica thin films

Sandrine Dourdain, Jean-François Bardeau, and Maggy Colas
*Laboratoire de Physique de l'Etat Condensé, UMR CNRS 6087, Université du Maine, 72085 Le Mans
 Cedex 09, France*

Bernd Smarsly
Max-Planck-Institute of Colloids and Interfaces, Am Mühlenberg, Potsdam D-14424, Germany

Ahmad Mehdi
*Laboratoire de Chimie Moléculaire et Organisation du Solide, UMR 5637 CNRS,
 Université de Montpellier II, Place E. Bataillon, F-34095 Montpellier Cedex 5, France*

Benjamin M. Ocko
Brookhaven National Laboratory, Department of Physics, Upton, New York, 119730-5000

Alain Gibaud^{a)}
*Laboratoire de Physique de l'Etat Condensé, UMR CNRS 6087, Université du Maine, 72085 Le Mans
 Cedex 09, France*

(Received 16 July 2004; accepted 17 February 2005; published online 11 March 2005)

Two-dimensional hexagonal silica thin films templated by a triblock copolymer were investigated by grazing incident small angle x-ray scattering (GISAXS) and x-ray reflectivity (XR) before and after removing the surfactant from the silica matrix. XR curves—analyzed above and below the critical angle of the substrate—are evaluated by the matrix technique to obtain the average electron density of the films, the wall thickness, the electron density of the walls, the radius of the pores, and subsequently the porosity of such mesoporous films. In combination with GISAXS, the surface area of the mesopores is ascertained, thereby providing a complete analysis of the porosity in thin films by x-ray scattering methods. © 2005 American Institute of Physics. [DOI: 10.1063/1.1887821]

In thin films, the nonintrusive determination of the surface area and of the porosity is a nontrivial issue.¹ Indeed, the BET technique that is used for powders is not applicable due to lack of materials. X-ray reflectivity (XR) that is sensitive to both the film average electron density and its profile can be used to determine the porosity of disordered films.^{2–5} The aim of this letter is to present the determination of the porous properties of a highly ordered silica thin film by a quantitative analysis of the XR. For this purpose, a silica matrix was initially templated by a polyethylene oxide/polypropylene oxide (PEO/PPO) triblock copolymer (with the commercial P123 name from BASF) that was removed by rinsing the film in ethanol.⁶ After rinsing, the film consisted of a regular array of cylindrical pores of diameter t_1 located at the nodes of a two-dimensional (2D) hexagonal lattice as shown in Fig. 1. By combining grazing incident small angle x-ray scattering (GISAXS) measurements with the XR analysis, we show how these parameters and the electron density of the silica matrix are obtained and further used to determine the porosity and the specific surface of the mesoporous film.

Films were made from initial sols prepared in two steps. First, 3.50 g of tetraethoxysilane (TEOS), 2.0 g of ethanol, and 2.5 g of H₂O (pH=1.25) were mixed and stirred at room temperature for 1 h. A second solution containing 1.2 g of P123 and 54.4 g of EtOH was then added to this sol. After 2 h of stirring, 4 g of H₂O (pH=1.25) was added. From the resulting sol, thin films were dip coated at a constant

withdrawal velocity of 14 cm/min on clean glass substrates in the final sol of molar composition 1 TEOS:72 C₂H₅OH:21 H₂O:0.022 HCl:0.012 P123. The composition of the sol was adjusted so as to make films about 100 nm thick. For the present study, two identical films were prepared at relative humidity around 60% and the temperature at 25 °C. One of the films was thoroughly rinsed in ethanol for 6 h to remove the surfactant so as to produce a mesoporous film and the other was not processed.

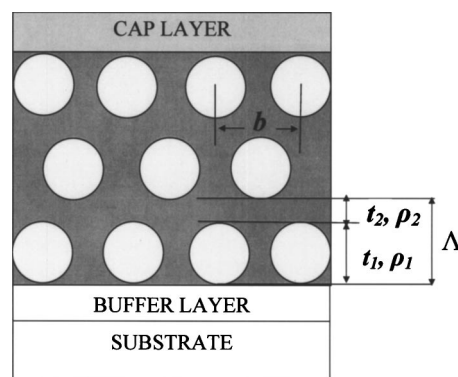


FIG. 1. Idealized model used to fit the reflectivity data. Films are considered to be made of Layer 1 either composed of surfactant/pores and silica (respectively, before rinsing and after rinsing) of thickness t_1 electron density ρ_1 , and a roughness σ_1 and of Silica layer 2 of thickness t_2 with an electron density ρ_2 , and a roughness σ_2 . The in-plane spacing between pores or micelles is denoted as b . For clarity, the figure shows only 3 layers out of the $N=8$ layers really present in the films. The roughness of the layers is not shown in the picture. Films are supported by a glass substrate and silica cap and buffer layers are also introduced in the model.

^{a)} Author to whom correspondence should be addressed; electronic mail: gibaud@univ-lemans.fr

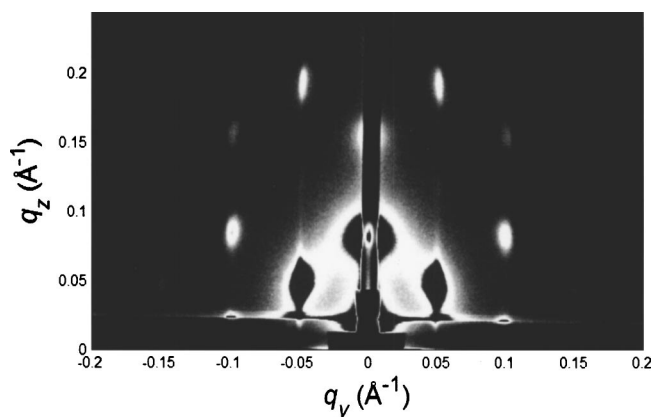


FIG. 2. GISAXS results of the rinsed film showing the 2D hexagonal structure.

XR was carried out with a wavelength of 1.54 Å on a Philips reflectometer. GISAXS was performed at the beamline X22B at the National Synchrotron Light Source, Brookhaven National Laboratory, using x rays with a wavelength of 1.567 Å. The exposure time was 10 s per frame and the incident angle was slightly higher than the critical angle of the substrate so that the film was still fully penetrated by the x rays.

Figure 2 shows the GISAXS pattern of the rinsed film. It exhibits the characteristic spots of the p6m 2D hexagonal symmetry and shows this symmetry is well preserved after rinsing.⁷ After rinsing, the intensity of the Bragg reflections increased as expected from a higher electron density contrast due to the removal of the surfactant from the silica matrix. This was further confirmed by the Raman analysis shown in Fig. 3. The signal of the H-C_{sp3} stretching bands related to the presence of P123 (or possibly to residual Si-OC₂H₅ groups) inside the film decreases drastically after rinsing. From the integrated intensity of these bands, one can conclude that about 91% of the CH₂ and CH₃ moieties were removed.

In Fig. 4, we show the two reflectivity curves for the initially prepared [Fig. 4(a)] and ethanol rinsed [Fig. 4(b)] films. As shown in the bottom insets of Fig. 4, two different

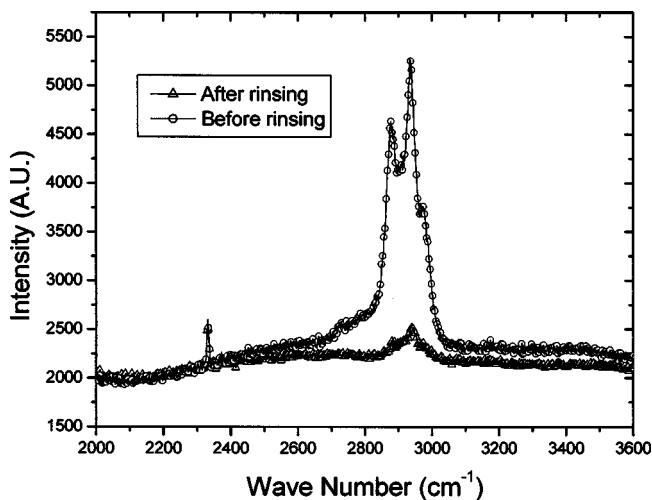


FIG. 3. Raman scattering experiments showing the disappearance of the H-C_{sp3} stretching bands located around 2900 cm⁻¹ that confirm the removal of the surfactant upon rinsing. The Raman signals are normalized to the nitrogen peak located at 2330 cm⁻¹.

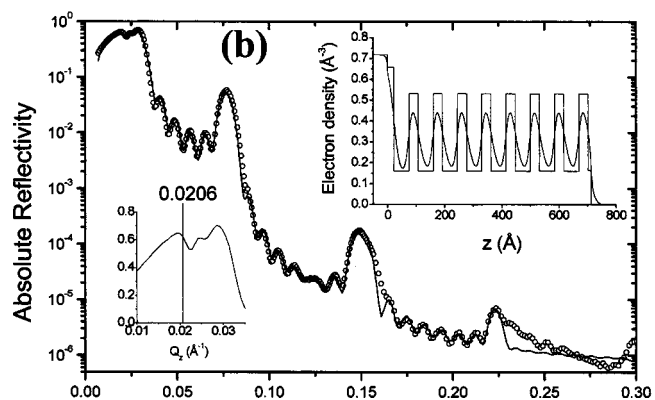
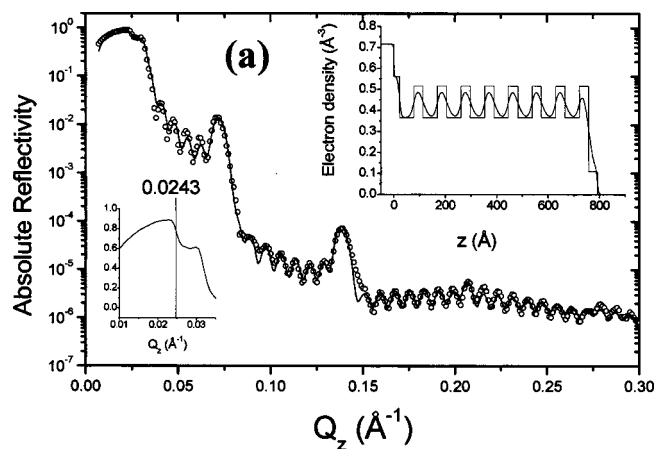


FIG. 4. Absolute reflectivity curves of the initial (a) and rinsed films (b). The top inset gives the electron density profile obtained from a fit via the matrix technique to the experimental data. The bottom inset shows a magnified view of the region below the critical angle. The value reported along the line is the average critical wave vector of the film. The modifications induced by the rinsing procedure are obvious both on the electron density profiles and on the average critical wave vector.

critical q_c are observed: The first one corresponds to the average electron density of the film, whereas the second one is that of the glass substrate ($\sim 0.0315 \text{ \AA}^{-1}$). As these films have an electron density lower than the substrate density, they actually act as quasi-waveguides.^{8,9} A comparison of the two panels clearly shows that removing the surfactant has a strong affect on the average electron density of the film. The shift of the critical vector, q_c , from 0.0243 \AA^{-1} to 0.0206 \AA^{-1} after rinsing is significant, meanwhile the substrate q_c remains the same for both samples. The reflectivity patterns, shown in Fig. 4, exhibit classical well-defined Kiessig fringes typical of uniform films of finite thickness both before and after rinsing. This suggests that the essential structure is not modified by the rinsing. The appearance of six fringes between each neighboring Bragg peaks indicates that the film is composed of eight layers with the same overall motif. The sharp Bragg peaks indicate a well-organized multilayer with a period $\Lambda = 9.0$ and 8.4 nm for the initial and rinsed films.

The experimental XR curves were calculated using the matrix technique.¹⁰ Our inferred profile adjusted by a least-squares fit to the data consisted of two stacked layers that were repeated $N=8$ times as shown in Fig. 1. In this model, the thickness t_1 defines both the radius of the surfactant micelle before rinsing and the pore diameter after rinsing. All of the parameters were adjusted by a fit to the experimental data and are reported in Table I. In agreement with the simple

TABLE I. Parameters obtained from the fits to the experimental data of the initial and rinsed films that were dip coated on a glass substrate. Films are made of Layer 1 either composed of surfactant/pores and silica (respectively, before rinsing and after rinsing) and of a pure silica Layer 2. These layers are repeated $N=8$ times. Cap and buffer layers of silica are also introduced in the model. For each layer, we adjust the critical wave vector q_c (namely, the electron density ρ), the interfacial roughness σ , and the thickness t . The first number is the one related to the initial film, while the second is the one for the rinsed film.

	Glass	Silica buffer	Layer 1	Layer 2	Silica cap
q_c (\AA^{-1})	0.032	0.0278/0.0302	0.0224/0.0149	0.0270/0.0273	0.012/0.015
ρ ($e^-/\text{\AA}^3$)	0.73 ^a	0.56/0.65	0.36/0.16	0.52/0.53	0.10/0.16
σ (\AA)	1.5 ^a	6.5/8	11.2/10.3	18.1/18.8	3.75/4.1
t (\AA)	—	22.9/22.4	55.6/52.9	36.1/32.4	33.7/10.1

^aParameter kept fixed during the fits.

Fourier decomposition of the periodic electron density of the stacking, we find that since the third peak is quite weak, $t_1 \cong 2t_2$. This yields a pore size and a wall thickness of about 6 nm and 3 nm, respectively.

The fitted density profiles (in the insets of Fig. 4) show how the electron density is modified by the removal of the surfactant while maintaining the $N=8$ sequence. It can be seen that in both films the silica walls (Layer 2) have a similar electron density. This shows that the rinsing procedure maintains the silica walls, thus providing a mesoporous film of good mechanical properties. The wall density, $0.52 e^-/\text{\AA}^3$, is however smaller than the one of bulk silica which is $0.72 e^-/\text{\AA}^3$.¹⁰ The electron density of porous Layer 1 exhibits, on the contrary, a drastic decrease from 0.36 to $0.14 e^-/\text{\AA}^3$ after rinsing as expected from the removal of the surfactant. From the parameters reported in Table I, one can calculate the average electron density $\langle \rho \rangle$ of each film and compare it to the unbiased experimental value measured at the critical angle of external reflection. The average electron density of the film is by definition.

$$\langle \rho \rangle = \frac{\rho_1 t_1 + \rho_2 t_2}{t_1 + t_2} = \frac{1}{4\pi r_e} \frac{q_{c1}^2 t_1 + q_{c2}^2 t_2}{t_1 + t_2}, \quad (1)$$

where $r_e = 2.8510^{-15}$ m is the classical radius of the electron. Substitution of the fitted parameters into Eq. (1) gives a density $0.30 e^-/\text{\AA}^3$ (i.e., $\langle q_c \rangle = 0.0206 \text{\AA}^{-1}$) for the rinsed film and $0.42 e^-/\text{\AA}^3$ (i.e., $\langle q_c \rangle = 0.0243 \text{\AA}^{-1}$) for the as deposited film. These calculated values are in perfect agreement with the experimental values of q_c shown in the bottom insets of Fig. 4. The fitting analysis for $q > q_c$ confirms the simple analysis of the average electron density obtained for $q < q_c$. After rinsing, the pore diameter was found to be 5.3 ± 1 nm.

Assuming that the pores are fully emptied during the rinsing procedure, the determination of the mesoporosity relates to the parameters t_1 , t_2 , ρ_1 , and ρ_2 by the following expression

$$\langle \Phi_{\text{meso}} \rangle = \frac{\rho_2 - \rho_1}{\rho_2} \frac{t_1}{t_1 + t_2} = \left(1 - \frac{q_{c1}^2}{q_{c2}^2} \right) \frac{t_1}{t_1 + t_2}. \quad (2)$$

From Eq. (2), it is found that the film has a mesoporosity, that is to say a volumic fraction of pores of 43% with an uncertainty of 5%. One can note that the porosity is also given by $\langle \Phi_{\text{meso}} \rangle = (\rho_2 - \langle \rho \rangle) / \rho_2$, a result that is fully consistent with Eq. (2) when substituting $\langle \rho \rangle$ by its expression [Eq. (1)].

The porosity is thus dictated by both the determination of average and of the silica wall electron densities. Since the silica wall electron density is less than the one of pure bulk silica, we can infer the walls exhibit some microporosity

given by $\langle \Phi_{\text{micro}} \rangle = (\rho_{\text{silica}} - \rho_2) / \rho_{\text{silica}}$, yielding a microporosity $\langle \Phi_{\text{micro}} \rangle = 28\%$ and an average mass density of the walls $\mu_{\text{wall}} = 1580 \text{ kg/m}^3$ that is less than the one of pure silica $\mu = 2200 \text{ kg/m}^3$.

The surface area $A = 103 \text{ m}^2/\text{g}$ of the mesopores, $A = \pi t_1 / \mu_{\text{wall}} (b(t_1 + t_2) - \pi t_1^2 / 4)$, was obtained from the parameters given in Table I and by the in-plane lattice parameter, $b = 13.5$ nm, deduced from the GISAXS measurements (Fig. 2).

We have shown that robust highly ordered silica thin films templated by P123 with a 2D hexagonal structure could be well preserved after the removal of the surfactant by rinsing in ethanol. This was clearly demonstrated by combining GISAXS, XR, and Raman scattering experiments. Based upon real space models of the electron density, we show how the meso- and microporosity of the rinsed films can be determined. The surface area associated with the mesopores is also ascertained from GISAXS measurements performed on the same films. Here, the pores were empty but they can be filled with many solvents. Besides the direct determination of the porosity, the method of analysis detailed in this letter now opens the route to the exploration of more fundamental aspects related to the porosity of materials, such as the understanding of nanowetting.

This work was supported by the French ACIS ‘‘Nanoscience’’ under projects ‘‘Nanoporomat’’ and ‘‘Autofyméhyopdir.’’ Work at Brookhaven National Laboratory is supported by U.S. DOE Contract No. DE-AC02-98CH10886.

¹G. C. Frye, A. Ricco, S. J. Martin, and J. C. Brinker, Mater. Res. Soc. Symp. Proc. **121**, 349 (1988).

²M. Klotz, N. Idrissi-Kandri, A. Ayril, A. van der Lee, and C. Guizard, J. Phys. IV **12**, 283 (2002).

³H. J. Lee, E. K. Lin, B. J. Bauer, W. L. Wu, B. K. Hwang, and W. D. Gray, Appl. Phys. Lett. **82**, 1084 (2003).

⁴J. J. Si, H. Ono, K. Uchida, S. Nozaki, H. Morisaki, and N. Itoh, Appl. Phys. Lett. **79**, 3140 (2001).

⁵A. Gibaud, A. Baptiste, D. A. Doshi, C. J. Brinker, L. Yang, and B. Ocko, Europhys. Lett. **63**, 833 (2003).

⁶The PEO and PPO blocks are soluble in ethanol; therefore, the rinsing procedure was chosen to avoid the large shrinkage or even worse the collapse of the oxide structure when the surfactant is removed by annealing.

⁷Note that in GISAXS, the footprint of the beam covers the entire length of the sample (here, 2.5 cm), so that the resulting pattern gives an averaged overview of the film structure.

⁸Y. P. Feng, S. K. Sinha, E. E. Fullerton, G. Grübel, D. Abernathy, D. P. Siddons, and J. B. Hastings, Appl. Phys. Lett. **67**, 3647 (1995).

⁹S. Lagomarsino, A. Cedola, S. Di Fonzo, W. Jark, V. Mocella, J. B. Pelka, and C. Riekel, Cryst. Res. Technol. **37**, 758 (2002).

¹⁰A. Gibaud, in *X Ray and Neutron Reflectivity: Principle and Applications*, edited by J. Daillant and A. Gibaud (Springer, Paris 1999), pp. 87–115.